

Numerical simulation and analysis of influencing factors for external prestressed reinforcement of bridges

External prestressing reinforcement belongs to active reinforcement field. Many researches on this technique have been done at home and abroad, but the numerical simulation is rare. In this paper, ANSYS is used to simulate the process of external prestressing reinforcement, and the influence of reinforcement method, effective prestress and reinforcement time on the reinforcement effect is analyzed. With the increase of tension-controlled stress, the reinforcement effect of simply supported beam is gradually enhanced, but the excessive tensile force can easily lead to the high stress state of anchoring end and external tendons, which is disadvantageous to the structure. With the delay of strengthening time, the cracking load and ultimate load are gradually reduced, and the reinforcement effect is gradually reduced. Therefore, in order to prolong the service life of the structure, it is necessary for the structure to carry on the timing inspection, discover the problem in time, and carry on the maintenance and reinforcement to the structure.

Keywords: Bridge; external prestressing reinforcement; numerical simulation ANSYS

1. Introduction

At home and abroad, a lot of researches have been carried out on the external prestressing reinforcement technology, including the study of the failure form of the strengthened beam, the calculation of the bearing capacity of the strengthened beam and the calculation of the stress of the external prestressed tendons^[1]. On the basis of a large number of experiments and analyses, a computational model is established, the limitation of which is that most of the experiments are based on trabecular tests, and the other is based on the theory of elastoplastic mechanics or nonlinear analysis^[2]. Its limitation is that the former has many hypotheses and is a simplified calculation method, while the latter is not fully considered for the nonlinear factors^[3-5]. In view of this, considering the material nonlinearity, the geometric nonlinearity and the state nonlinearity of the structure, the mechanical analysis of the external prestressing reinforcement system is carried out, and the actual reinforcement process is simulated^[6]. The mechanism of external reinforcement and

the influence of different parameters on the reinforcement effect are studied^[7]. The research method is convenient and practical, and can be extended to the reinforcement simulation of existing bridges, in order to calculate the bridge reinforcement project more accurately, which has good research value and engineering significance^[8].

2. Mechanical analysis of external prestressed reinforcement system

The distribution of internal force of bridge structure must be considered in the arrangement of external prestressed tendons^[9]. The position can be arranged on the outside or inside of the beam according to the structure and section form of the original structure. The integral calculation schema is an internal statically indeterminate structure^[10-12]. According to its stress characteristics, the reinforcement system can be divided into prestressing stage and live load stage.

- (1) Prestressing stage: when the tensile horizontal tendons reach the control stress, the horizontal tendons are anchored. The oblique bars are connected with horizontal tendons through sliding blocks. The horizontal forces caused by oblique tendons have eccentric pressure on the beam body, and the vertical forces have negative bending moment and negative shear forces on the beam body.
- (2) The stage of live load action: the beam body will bend and deform after the live load action, which will increase the tensile force in the horizontal reinforcement, the tension in the oblique bar, the positive pressure of the cushion to the beam body and the friction force.

The structural mechanics method can be used to solve the simply supported beams strengthened with external cables, and the overall calculation schema is shown in Fig. 1.

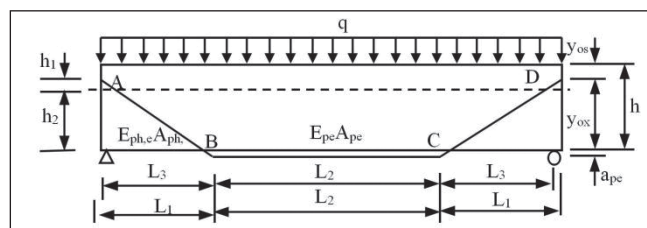
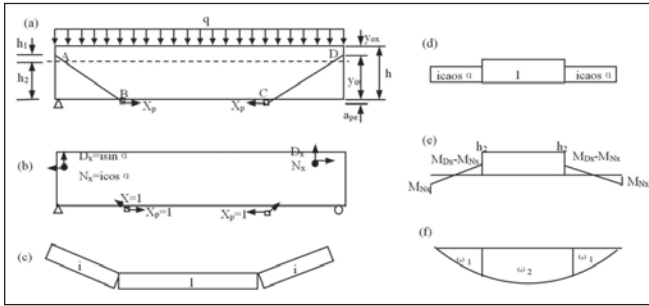


Fig. 1: Integral calculation of simply supported beams strengthened with external cables

Mr. Li Jun, School of Civil Engineering, Changsha University of Science and Technology, Changsha, China.

When the external prestressed reinforcement system is solved by force method, the horizontal tension increment caused by live load is taken as the basic variable, and the basic structure is obtained by cutting off the horizontal reinforcement. The calculation schema is shown in Fig. 2.



(a) Basic structure of force method (b) unit force diagram (c) In vitro force bar N1 diagram (pull as positive) (d) Beam N₁ diagram (positive with pressure) (e) M₁ diagram of beam (the lower edge is drawn as positive) (f) M_p diagram of beam body (the following edges are drawn as positive)

Fig. 2. Calculation schema by force method

In the picture:

- q – live load set.
- ω_1 – The area of bending moment diagram with variable action from the center of the cushion to the center of the support.
- $\omega_1 = \frac{1}{2} q l_3^2 \left(\frac{L}{2} - \frac{l_3}{2} \right)$
- ω_2 – Area of bending moment diagram with variable action in the center of two cushion plate.
- $\omega_2 = \frac{1}{12} q l^3 - q l_3^2 \left(\frac{L}{2} - \frac{l_3}{2} \right)$
- y_1 – Vertical coordinates of the center of gravity of the area of bending moment diagram generated by unit force at the end of the beam. $y_1 = (l_1 - x_c) A \sin \alpha$
- x_c – Distance between centre of gravity of ω_1 graph and center of pad.
- $x_c = \frac{l_3(2L - l_3)}{6L - 4l_3}$
- $\lambda = \frac{1}{\cos \theta_c + f_0 \sin \theta_c}$
- f_0 – Friction coefficient between slider and beam bottom
- α – Angle between oblique reinforcement and longitudinal axis of beam
- a – Horizontal distance of anchoring point from zero point to anchorage point of bending moment at the end of beam caused by unit force
- b – The horizontal distance between the moment zero at the end of the beam and the center of the plate caused by the unit force

By cutting off the horizontal tendons and replacing them with superfluous constraints X₁, the equation of force method

is as follows:

$$\delta_{11} X_p + \Delta_{1p} = 0 \quad (1)$$

Ignoring the axial deformation and shear deformation of the beam, the calculated Δ_{1p} is as follows:

$$\Delta_{1p} = \sum \int \frac{\bar{M}_1 M_p}{EI} dx = \frac{1}{EI_0} (2\omega_1 \lambda \cos \theta_c - 2\omega_1 y_1 - \omega_2 h_2) \quad (2)$$

δ_{11} calculated by the following formula

$$\delta_{11} = \sum \int \frac{\bar{N}_1^2}{EA} dx + \sum \int \frac{\bar{M}_1^2}{EI} dx \quad (3)$$

Of which:

$$\sum \int \frac{\bar{N}_1^2}{EA} dx = \frac{2\lambda^2 l_1}{E_{pbc} A_{pbc} \cos \alpha} + \frac{l_2}{E_{pc} A_{pc}} + \frac{1}{E_c A_0} (2\lambda^2 l_1 \cos^2 \alpha + l_2) \quad (4)$$

$$\sum \int \frac{\bar{M}_1^2}{EI} dx = \frac{1}{EI_0} \left[\frac{2}{3} a M_{Nx}^2 + \frac{2}{3} b (M_{Dx} - M_{Nx})^2 + l_2 h_2^2 \right] \quad (5)$$

By replacing the above results with the equation of force method, the formula of tension increment of horizontal force bar can be obtained as follows:

$$X_p = -\frac{\Delta_{1p}}{\delta_{11}} = f(A_{p,c}, q) \quad (6)$$

It can be seen from the formula 6 that if the size of the beam, the structure and the material of the external cable are known, the tensile force increment in the external cable horizontal tendon can be calculated by the upper formula. The magnitude of the tensile force increment is mainly related to the area of the horizontal tendon and the live load set degree of the action.

3. Simulation of reinforcement process of reinforced concrete beam

3.1. COMPUTATIONAL PURPOSE

- (1) Combined with the finite element analysis software ANSYS, the effect of different arrangement of external reinforcement on the reinforcement effect is studied. The reinforcement methods are as follows: no steering block, one steering block in the middle of the span, and one steering block one third of the span from each side of the support.
- (2) By adjusting different tensioning control stress, the influence of effective prestress on reinforcement effect is studied. The range of tension-controlled stress is between $0.3f_{pk} \sim 0.6f_{pk}$.
- (3) By setting different load steps and controlling the application time of prestressing force, the influence of different reinforcement time on the reinforcement effect is studied.

3.2. ESTABLISH REINFORCEMENT MODEL

The reinforcement model is based on simply supported beam, and the load is 27.6kN when the deflection value

reaches $L/600$. Therefore, the load values of this magnitude are applied separately in the first load step calculated below. The external tendons are $2\Phi 15.20$, and their performance parameters are shown in Table 1. The tensile control force σ_{con} is $0.4f_{pk}$, the temperature drop is $T = 316^{\circ}\text{C}$, and the finite element model is shown in Figs. 1~3.

TABLE 1. MATERIAL PERFORMANCE TABLE

Sheet of mechanical properties of steel					
Diameter (mm)	Area (mm ²)	Yield strength (Mpa)	Modulus of elasticity (Mpa)	Poisson ratio	Density (t/mm ³)
Φ14	308	360	2.28E+05	0.3	7.85E-09
Φ12	226	360	2.25E+05	0.3	7.85E-09
Φ8	50.3	240	2.00E+05	0.3	7.85E-09
Φs15.2	280	1581	2.00E+05	0.3	7.87E-09
Table of mechanical properties of concrete					
Grade	Compression strength (Mpa)	Tensile strength (Mpa)	Modulus of elasticity (Mpa)	Poisson ratio	Density (t/mm ³)
C30	27.6	2.6	2.9E+04	0.2	2.50-09

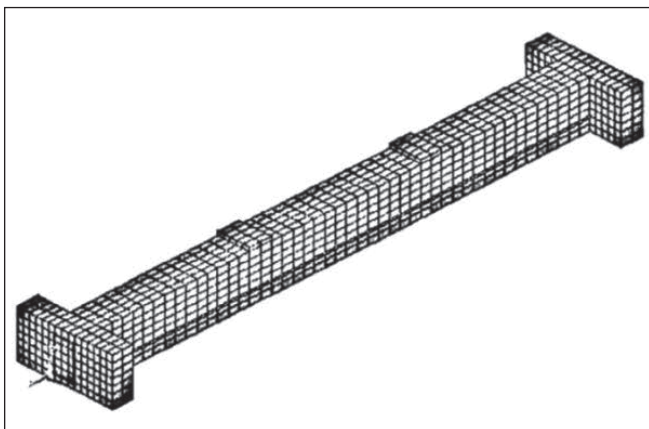


Fig. 1: simply supported beam strengthened with external cables of linear form

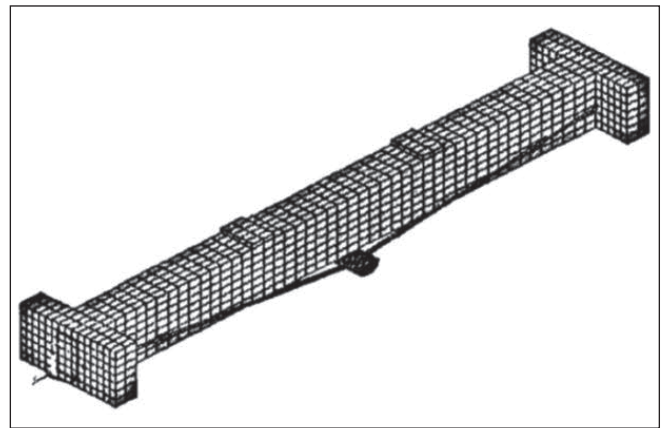


Fig. 2: simply supported beam strengthened with external cables of broken lines

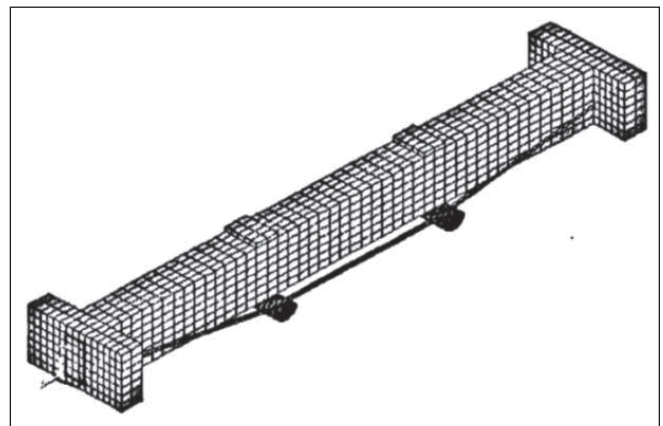


Fig. 3: simply supported beam strengthened with double broken external cables

4. Comparative analysis of influencing factors of reinforcement effect

4.1. INFLUENCE OF REINFORCEMENT PATTERN ON REINFORCEMENT EFFECT

According to the established model, each type of reinforcement is reinforced when the deflection reaches $L/600$. The concrete calculation results are given in Tables 2~5.

TABLE 2. COMPARISON TABLE OF CALCULATION RESULTS

Reinforcement form	Cracking load (kN)	Ultimate load (kN)	Stress increment of external tendons (Mpa)	Tensile reinforcement stress (Mpa)	Compressive steel bar stress (Mpa)	Deflection (mm)
No steering block	38.9	117.0	168.2	360	-259.3	9.1
A steering block	64.6	175.2	354.2	360	-323.1	9.9
Two steering blocks	73.2	195.6	422.1	360	-301.3	10.1

1. No steering block

TABLE 3. CALCULATION RESULTS OF EXTERNAL REINFORCEMENT WITHOUT STEERING BLOCK ($f=L/600$)

Load step number	Load (kN)	Stress increment of external tendons (Mpa)	Tensile reinforcement stress (Mpa)	Compressive steel bar stress (Mpa)	Deflection (mm)
1	27.6		203.4	-48.0	3.8
2	27.6		-25.1	-50.0	0.2
3	0	0	-63.9	-13.1	-1.0
	8.9	3.7	-54.1	-24.8	-0.6
	20.0	8.3	-39.0	-39.4	-0.1
	38.9	16.0	-18.3	-65.5	0.6
	45.2	19.1	-0.3	-75.8	1.0
	51.5	23.6	16.5	-88.5	1.4
4	64.1	37.7	68.8	-118.1	2.5
	76.7	56.3	134.0	-148.1	3.8
	89.3	77.6	205.3	-180.1	5.3
	95.0	88.2	238.5	-194.8	6.0
	103.5	106.8	285.6	-220.0	7.2
	117.0	133.6	360	-259.3	9.1

Note: cracking load 38.9kN

2. A steering block

TABLE 4. CALCULATION RESULTS OF EXTERNAL REINFORCEMENT OF ONE STEERING BLOCK ($f=L/600$)

Load step number	Load (kN)	Stress increment of external tendons (Mpa)	Tensile reinforcement stress (Mpa)	Compressive steel bar stress (Mpa)	Deflection (mm)
1	27.6		188.3	-48.8	3.9
2	27.6		-69.2	29.6	-1.1
3	0		-109	182.4	-4.0
	8.2	10.4	-98.5	130.9	-3.1
	28.6	28.9	-72.5	30.2	-1.3
	46.6	47.7	-46.1	-14.9	-0.4
	64.6	73.1	-22.7	-40.6	0.3
	82.6	100.9	10.8	-74.4	1.2
4	109.6	141.9	93.7	-126.8	3.3
	127.6	182.4	163.2	-163.8	4.9
	145.6	224.9	235.1	-211	6.7
	163.6	260.6	310.4	-265.7	8.6
	175.2	285.7	360	-303.2	10.4

Note: cracking load 64.6kN

3. Two steering blocks

TABLE 5. CALCULATION RESULTS OF EXTERNAL REINFORCEMENT OF TWO STEERING BLOCKS ($f=L/600$)

Load step number	Load (kN)	Stress increment of external tendons (Mpa)	Tensile reinforcement stress (Mpa)	Compressive steel bar stress (Mpa)	Deflection (mm)
1	28.8		200.1	-49.6	4.1
2	28.8		-75.9	35.3	-1.4
3	0	0	-124.7	208.3	-5.0
	9.3	26.9	-113.2	147.3	-3.9
	22.2	52.6	-95.3	72.5	-2.5
	42.6	85.2	-65.2	-6.3	-0.9
	63.0	106.6	-41.3	-34.5	-0.1
	73.2	117.6	-30.5	-48.3	0.3
4	83.4	130.8	-11.5	-63.2	0.7
	103.8	166.8	47.3	-98.3	1.9
	124.2	215.1	116.5	-136.5	3.5
	144.6	268.5	188.6	-176.2	5.1
	165.0	325.4	263.5	-218.6	6.9
	185.4	385.8	343.2	-270.5	8.8
	195.6	422.1	360.2	-301.5	10.1

Note: cracking load 73.2kN

The following conclusions can be drawn from the analysis of Tables 2~5:

- (1) Bearing capacity: it can be seen from the cracking load and ultimate load after reinforcement that the external cable is used to reinforce the existing simply supported beam, no matter which reinforcement method is used, the cracking load and ultimate load of the beam body are greatly increased. Especially, the ultimate bearing capacity after reinforcement is 3.3 times and 3.6 times of that before reinforcement. The mechanical behaviour of beam is improved fundamentally. On the one hand, it is considered that the steering gear increases the midspan force arm of the beam, and on the other hand, the force arm decreases with the increase of deflection of the beam, which results in the loss of resistance moment.
- (2) Stress of steel bar: it can be seen from the stress value of the bottom steel bar in Tables 2 ~ 5 that at the initial stage of beam loading, the lower steel bar is under tension and the upper steel bar is under compression. After the prestress is applied, the stress state of the beam body changes from the upper compression state to the lower compression state because the prestress counteracts the effect of the original load. At the same time, the tensile stress appears in the steel bar in the upper part of the beam body. The compressive stress appears in the lower edge of the non-prestressed steel

bar. With the increase of the load, the lower part of the beam is cracked again, the deflection of the beam is larger than that of the reverse arch, and gradually increases, the tension stress appears again in the steel bar at the lower edge and the compressive stress in the upper steel bar. This coincides with the actual recipient state. At the same time, it can be seen that under the same load, the stress of the tensile steel bar without steering block is larger than that of the steel bar with steering block, and the increment of external tendon is much smaller than that without steering block, so the utilization ratio of external tendon can be improved by setting steering block. Although the external tendon increment of two steering blocks is higher than that of one steering block, the degree of improvement is not obvious, which indicates that the adverse effect of secondary effect can be effectively reduced by setting steering device.

- (3) Span deflection: from the deflection values listed in the table, it can be seen that after reinforcement, the beam appears the reverse arch due to the effect of external prestress. The reverse arch value with two steering blocks is the largest, and the reverse arch value with no steering block is small, which further shows that setting steering block can improve the reinforcement effect of external cable on beam body. After unloading, the inverse arch value of beam body increases further, and the

maximum value reaches 5.0 mm. The deflection curves of the beams are still approximately straight lines after cracking, which indicates that the strengthened beams are still in the elastic working state in a certain period after cracking. At the same time, the stiffness of the beam body is increased with the application of prestressing, so that the deflection of the beam body decreases with the increase of load, and the deflection after strengthening under the same load decreases obviously. The deflection value of the reinforcement mode with steering device is obviously lower than that of the strengthening mode without steering device.

- (4) Stress increment: it can be seen from the above diagram that the stress increment and ultimate stress are the smallest compared with other reinforcement methods, although the prestressing loss is relatively small. It is shown that the secondary effect is the most obvious and the utilization efficiency of the material is low when the beam body is strengthened with linear external cables.

In addition, it can be seen from the above curve that the stress increment of prestressed tendons is closely related to the mid-span deflection of members, regardless of the line shape of external tendons.

- (5) Through the analysis of the results of strengthening simply supported beams with external tendons, it can be seen that when the beam is damaged by external prestressed reinforcement, the upper reinforcement and external cables do not reach the yield stress, so it is a brittle failure.

4.2. EFFECT OF EFFECTIVE PRESTRESS ON REINFORCEMENT EFFECT

In order to study the effect of effective prestress on the reinforcement effect, the tension-controlled stress σ_{con} is taken as the parameter and the variable range is $474.3\text{MPa}(0.3f_{pk})$ to $948.6\text{MPa}(0.6f_{pk})$. Table 6~9 shows the calculated results of strengthening with different tensioning control stresses when the deflection reaches $L/600$.

TABLE 6. COMPARISON OF CALCULATION RESULTS

Reinforcement form	Cracking load (kN)	Ultimate load (kN)	Stress increment of external tendons (Mpa)	Tensile reinforcement stress (Mpa)	Compressive steel bar stress (Mpa)	Deflection (mm)
$\sigma_{con} = 0.3f_{pk}$	37.6	139.5	350.6	360	-256.7	10.1
$\sigma_{con} = 0.4 f_{pk}$	64.6	175.2	332.7	360	-323.1	9.7
$\sigma_{con} = 0.5 f_{pk}$	65.7	183.0	318.5	360	-329.5	9.5
$\sigma_{con} = 0.6 f_{pk}$	83.4	201.0	295.5	360	-360	9.2

TABLE 7. CALCULATION RESULTS OF DIFFERENT TENSILE STRESS REINFORCEMENT ($0.3f_{pk}$)

Load step number	Load (kN)	Stress increment of external tendons (Mpa)	Tensile reinforcement stress (Mpa)	Compressive steel bar stress (Mpa)	Deflection (mm)
1	27.6		188.3	-48.8	3.9
2	27.6		-165	-22.2	0.0
3	0		-56	86.8	-1.9
	8.2	11.4	-45	42.5	-1.1
	28.6	33.1	-16.5	-22.9	0.0
	37.6	40.7	-8.1	-32	0.3
	55.6	67.2	34.7	-57.3	1.4
	64.6	86.6	65.4	-72	2.1
4	73.6	108.3	98.8	-87.7	2.9
	82.6	130.9	133.4	-103.7	3.9
	109.6	203.3	239.3	-152.8	6.8
	127.6	257.5	311.2	-194.3	8.7
	136.6	284.5	348.7	-219.9	9.7
	139.5	293.3	360	-256.7	10.1

Note: cracking load 37.6kN

TABLE 8. CALCULATION RESULTS OF DIFFERENT TENSILE STRESS REINFORCEMENT ($0.5f_{pk}$)

Load step number	Load (kN)	Stress increment of external tendons (Mpa)	Tensile reinforcement stress (Mpa)	Compressive steel bar stress (Mpa)	Deflection (mm)
1	27.6		188.3	-48.8	3.9
2	27.6		-70.4	40.4	-1.3
3	0	0	-118.3	197	-4.4
	0.9	1.4	-117.1	191.6	-4.3
	13.0	20.0	-101.5	117.3	-3.0
	29.1	42.5	-72.2	39.8	-1.6
	47.4	61.5	-53.8	-32.9	-0.6
	65.7	77.0	-28	-52	0.1
4	84.0	97.5	0.6	-74.2	1.0
	102.3	128.6	47.9	-107.8	2.2
	120.6	169.5	111.5	-144	3.8
	157.2	268.7	258.2	-244.3	7.2
	175.5	322.3	336.2	-301.4	8.9
	183.0	347.7	360	-329.5	9.5

Note: cracking load 65.7kN

TABLE 9. CALCULATION RESULTS OF DIFFERENT TENSILE STRESS REINFORCEMENT ($0.6f_{pk}$)

Load step number	Load (kN)	Stress increment of external tendons (Mpa)	Tensile reinforcement stress (Mpa)	Compressive steel bar stress (Mpa)	Deflection (mm)
1	27.6		188.3	-48.8	3.9
2	27.6		-102.5	80.8	-2.3
3	0	0	-134.3	257.3	-5.9
	1.0	1.6	-133.2	250.9	-5.7
	14.5	23.1	-118.6	166.3	-4.1
	32.4	49.2	-100.8	72.7	-2.4
	42.6	61.7	-89.9	34.1	-1.7
	63.0	81.6	-70.5	-44.2	-0.7
4	83.4	99.9	-51.9	-66.7	0.2
	103.8	124.5	-5.1	-92.9	1.2
	124.2	159.6	49.7	-131.9	2.6
	144.6	205.7	123.7	-176.4	4.4
	165.0	259.1	205.5	-234.9	6.3
	185.4	318.2	291.1	-302.6	8.0
	201.0	379.2	360	-360	9.2

Note: cracking load 83.4kN

The following conclusions can be drawn from the above results:

- (1) With the increase of tension control stress, the cracking load and ultimate load of simply supported beam are greatly increased. When the tensile force is increased from $0.3f_{pk}$ to $0.6f_{pk}$, the cracking load is increased

from 37.6kN to 83.4 kN, and the ultimate load is increased from 139.5kN to 201kN. It is concluded that the greater the prestressing force is, the greater the equivalent load will be, and the higher the normal section strength will be after reinforcement, the more obvious the reinforcement effect will be.

- (2) Under the same load, the deflection of beam decreases with the increase of tensioning control stress. The analysis shows that the greater the tension control stress, the greater the external load moment counteracted. Under the same load, the smaller the bending moment of beam body is, the larger the stiffness of beam body is, and the smaller the deflection is. It shows that prestress reinforcement has good reinforcement. However, the prestressing loss of external prestressed tendons is smaller than that of common prestressed concrete beams, so the tension control stress of external tendons should not be too high. The Anchorage end and the prestressed tendons are in high stress state for a long time, which results in the sudden destruction of the structure.
- (3) At the beginning of loading, the stress increment is basically the same. However, with the increase of load, low tensile force will result in higher stress increment. It shows that the ultimate stress increment of external cables decreases gradually with the increase of tensioning control stress.
- (4) When the tensile force is 0.4f_{pk} and 0.5 f_{pk}, the reinforcement effect is close, the crack load and ultimate load are increased, and the upper part of the beam is cracked within the acceptable range. Comprehensive comparison shows that the tension control between 0.4 f_{pk} and 0.5 f_{pk} is more suitable for this simply supported beam.

4.3. EFFECT OF REINFORCEMENT TIME ON REINFORCEMENT EFFECT

In order to study the effect of different reinforcement time on the reinforcement effect, this paper studies the flexural reinforcement method with a steering device. Through the birth and death element to control the application time of prestress, the external cable is activated when the deflection reaches 0, L/1100, L/600, L/500, L/300, and the prestressing force is applied to the beam body. The following are the results of the calculation. The calculated results of beam deflection up to L/600 are given in Table 3.

An analysis of Table 10 leads to the following conclusions:

- (1) Bearing capacity: when the beam is strengthened after deflection reaches L/600, the cracking load and ultimate load are lower than that before the deflection reaches L/600. Compared to f=L/300, the cracking load of f=0 is reduced from 114.0kN to 61.9kN, and the crack load is reduced to 45.7kN. The ultimate load 195.6kN is reduced to 165.4kN, and the ultimate load is reduced to 18.3kN.
- (2) Stress of reinforcement: under the same load, the stress of reinforcing bar and the stress increment of external reinforcement increase gradually with the delay of reinforcement time. It is considered that when the deformation of the beam is large, the neutral axis of the beam is not obviously reduced, and the compressive area of the concrete is not increased, because of the larger damage degree of the beam body, and the reduction of the neutral axis of the beam body is not obvious after strengthening the beam body. The tensile force increment of steel bars and external tendons in tension zone will bear greater external torque, so the reinforcement and external tendons will show greater stress value.
- (3) Span deflection: under the same load, with the extension of reinforcement time, the mid-span deflection of beam body increases gradually, but the ultimate deflection decreases obviously. It is considered that the stiffness of the beam is not much increased when the deformation of the beam is large, which leads to the large deformation of the beam under the same load. Comparing the reinforcement effect of beam with different reinforcement time, it can be seen that with the delay of strengthening time, the reinforcement effect is gradually decreasing. Therefore, in order to prolong the service life of the structure, it is necessary for the structure to carry on the timing inspection, to realize the problem early, and to carry on the maintenance and reinforcement of the structure as early as possible.

5. Conclusions

In this paper, numerical simulation and research on external prestressing reinforcement are carried out, and the effects of different arrangement of external cables, different prestressing

TABLE 10. COMPARISON OF CALCULATION RESULTS

Reinforcement form	Cracking load (kN)	Ultimate load (kN)	Stress increment of external tendons (Mpa)	Tensile reinforcement stress (Mpa)	Compressive steel bar stress (Mpa)	Deflection (mm)
f=0	114.0	195.6	376.4	360	-360	11.0
f=L/1100	100.8	183.0	343.6	360	-360	10.3
f=L/600	64.6	175.2	332.7	360	-323.1	9.7
f=L/500	61.9	165.4	329.9	360	-303.4	9.6
f=L/300	55.6	160.5	315.4	360	-275.1	9.2

force and different reinforcement time on reinforcement effect are analyzed. The conclusions are as follows:

- (1) In the case of tri-point loading, the cracking load and ultimate load of beam are greatly increased, regardless of the reinforcement method. Especially, the ultimate bearing capacity after reinforcement is 3.33.6 times of that before reinforcement. The bending property of the beam is improved fundamentally.
- (2) With the increase of tension-controlled stress, the stress increment and deflection of the external cable are relatively reduced under the same load, although the cracking load and the ultimate load of the simply supported beam are greatly increased. Therefore, it is shown that the tension control force is not as large as possible and not as small as possible when the beam is strengthened. It should be adjusted appropriately according to the specific conditions, and the tension control of the simply supported beam is more appropriate between $0.4f_{pk} \sim 0.5f_{pk}$.
- (3) Compared to the reinforcement effect of different strengthening time, when the beam deformation is small, the cracking load and the ultimate load are higher than that of the deformation. It shows that the reinforcement effect decreases gradually with the delay of reinforcement time. Therefore, in order to prolong the service life of the structure, it is necessary for the structure to carry on the timing inspection, to realize the problem early, and to carry on the maintenance and reinforcement of the structure as early as possible.

References

1. Ren W, Sneed L H, Yang Y, et al (2015): "Numerical Simulation of Prestressed Precast Concrete Bridge Deck Panels Using Damage Plasticity Model". *International Journal of Concrete Structures & Materials*, 9(1), 45-54.
2. Han J, Song Y, Wang L, et al (2015): "Residual strain analysis of non-prestressed reinforcement in PPC beams under fatigue loading". *Materials & Structures*, 48(6), 1785-1802.
3. Sritharan S, Cox A M, Huang J, et al (2016): "Minimum confinement reinforcement for prestressed concrete piles and a rational seismic design framework". *Pci Journal*, 61(1), 51-69.
4. Choun Y S, Park J (2015): "Evaluation of seismic shear capacity of prestressed concrete containment vessels with fiber reinforcement". *Nuclear Engineering & Technology*, 47(6), 756-765.
5. Hussain Q, Pimanmas A, Hussain Q, et al (2015): "Shear Strengthening of RC Deep Beams with Sprayed Fiber-reinforced Polymer Composites (SFRP): Part 2 Finite Element Analysis". *Latin American Journal of Solids & Structures*, 12(7), 1266-1295.
6. Liu X G, Fan J S, Nie J G, et al (2015): "Experimental and analytical studies of prestressed concrete girders with corrugated steel webs". *Materials & Structures*, 48(8), 2505-2520.
7. Bazne M O A, Vahedifard F, Shahrokhbadi S (2015): "The Effect of Geonet Reinforcement on Bearing Capacity of Low-Compacted Soft Clay". *Transportation Infrastructure Geotechnology*, 2(1), 47-63.
8. Hajali M, Alavinasab A, Shdid C A (2015): "Effect of the location of broken wire wraps on the failure pressure of prestressed concrete cylinder pipes". *Structural Concrete*, 16(2), 297-303.
9. Sun R, Sevillano E, Perera R (2015): "A discrete spectral model for intermediate crack debonding in FRP-strengthened RC beams". *Composites Part B Engineering*, 69(2015), 562-575.
10. Wang G, Liu C, Jiang Y, et al (2015): "Rheological Model of DMFC Rockbolt and Rockmass in a Circular Tunnel". *Rock Mechanics & Rock Engineering*, 48(6), 2319-2357.
11. Schneider R, Fischer J, Bügler M, et al (2015): "Assessing and updating the reliability of concrete bridges subjected to spatial deterioration – principles and software implementation". *Structural Concrete*, 16(3), 356-365.
12. DENG Libin, WU Fangbo, ZHOU Xuhong (2015): "Parametric analysis of fire-resistant behavior of prestressed precast component composite slab". *Fire Safety Science*, 51(12), 2816-2817.

ANALYSIS ON PRICE VOLATILITY BETWEEN WTI LIGHT CRUDE AND RAW COAL

Continued from page 673

6. Bertrand Rioux, Philipp Galkin, Frederic Murphy, et al. (2017): "How do price caps in China's electricity sector impact the economics of coal, power and wind? Potential gains from reforms". *Energy Journal*, 38, 63-75.
7. Julien Chevallier. (2013): "Price relationships in crude oil futures: new evidence from CFTC disaggregated data". *Environmental Economics & Policy Studies*, 15(2), 133-170.
8. Zhihua Ding, Lingyun Hea, Caicai Feng, et al. (2016): "The impact of coal price fluctuations on China's economic output". *Applied Economics*, 48(24), 2225-2237.

ANALYSIS ON SUSTAINABLE PERFORMANCE OF WIND POWER BY USING MCDM METHOD

Continued from page 680

9. Zyoud Shaher H., Fuchs-Hanusch Daniela (2017): "A bi-biometric-based survey on AHP and TOPSIS techniques", *Expert Systems with Applications*, 78, 158-181.
10. Brahim Haddad, Abdelkrim Liazid, Paula Ferreira (2017): "A multi-criteria approach to rank renewables for the Algerian electricity system", *Renewable Energy*, 107, 462-472.
11. Geovanna Villacreses, Gabriel Gaona, Javier Gomez, Diego Jijon (2017): "Wind farms suitability location using geographical information system (GIS), based on multi-criteria decision making (MCDM) methods: The case of continental Ecuador", *Renewable Energy*, 109, 275-286.
12. Fausto Cavallaro, Luigi, Ciralo (2005): "A multicriteria approach to evaluate wind energy plants on an Italian island", *Energy Policy*, 33, 235-244.